Geochemistry Geophysics Geosystems G3
AN ELECTRONIC JOURNAL OF THE EARTH SCIENCES
Published by AGU and the Geochemical Society

Article
Volume 10, Number 1
31 January 2009
Q01012, doi:10.1029/2008GC002234
ISSN: 1525-2027

Migration imaging and forward modeling of microseismic noise sources near southern Italy

Keith Brzak, Yu Jeffrey Gu, and Ahmet Ökeler
Department of Physics, University of Alberta, Edmonton, Alberta T6G 2G7, Canada (kbrzak@ualberta.ca)

Michael Steckler and Arthur Lerner-Lam
Lamont Doherty Earth Observatory of Columbia University, Route 9W, Palisades, New York 10964, USA

[1] This study combines migration and forward source modeling techniques to examine the existence and location of persistent seismic noise near southern Italy. Our results demonstrate that noise source modeling is both feasible and recommended in validating the "ambient source" assumption prior to noise-based velocity analyses. Persistent noise sources near the Gargano promontory and the Tyrrhenian Sea coast are strongly suggested by the observed cross-correlations. The presence of a single point source or a cluster of point sources could both produce coherent Rayleigh wave energy in southern Italy. While the nature of the noise sources is still uncertain, baroclinic estimates and dynamic topography models favor an explanation that encompasses atmosphere-ocean coupling and heightened wave interaction off the Adriatic coast. Our records indicate that these noise sources can maintain their average location for up to 7 months despite seasonal and, possibly, daily variations.

Components: 6865 words, 13 figures.

Keywords: ambient noise; southern Italy; Gargano; source migration; CAT/SCAN.

Index Terms: 7299 Seismology: General or miscellaneous.

Received 8 September 2008; **Revised** 10 November 2008; **Accepted** 10 December 2008; **Published** 31 January 2009.

Brzak, K., Y. J. Gu, A. Ökeler, M. Steckler, and A. Lerner-Lam (2009), Migration imaging and forward modeling of microseismic noise sources near southern Italy, *Geochem. Geophys. Geosyst.*, *10*, Q01012, doi:10.1029/2008GC002234.

1. Introduction

[2] Techniques based on the correlation of seismic noise have been increasingly popular in the tomographic imaging of crust and upper mantle structures in recent years. The theory behind these techniques underwent stages of development since the connections between reflection seismograms and autocorrelation functions was first documented in studies of plane waves in layered medium over 40 years ago [e.g., *Kunetz and d'Erceville*, 1962; *Claerbout*, 1968]. Following an expansion of the original hypothesis to what is presently referred to as "Clarebout's conjecture" [*Rickett and Claerbout*, 1999], the presence of the seismic response in time domain cross-correlation functions was validated both in theory [*Lobkis and Weaver*, 2001] and in observations of unfiltered seismic coda waves [*Campillo and Paul*, 2003]. Subsequent studies using reciprocity and scattered waves [*Wapenaar et al.*, 2004; *Snieder*, 2004] led to increased confidence in tomographic maps under the assumption of "ambient" noise sources [*Sabra et al.*, 2005b; *Shapiro et al.*, 2005; *Yao et al.*, 2006; *Cho et al.*, 2007; *Gudmundsson et al.*, 2007; *Lin et al.*, 2007;

Moschetti et al., 2007; *Lin et al.*, 2008]. Devoid of dominant, nonuniform noise sources, Green's functions can be sufficiently extracted from both surface [e.g., *Sabra et al.*, 2005a; *Snieder*, 2004] and body [*Roux et al.*, 2005] waves after averaging months to years of continuous seismic records.

[3] Imaging seismic velocities using noise is not as straightforward as conventional earthquake-based analyses, however. Contamination during the retrieval of Green's functions may arise from accidental inclusions of large-amplitude earthquake signals or from unevenly distributed noise sources near the region of interest. While the influence of earthquakes can be sufficiently suppressed by removing known events based on published catalogs, one-bit normalization, and spectral whitening [*Bensen et al.*, 2007], the existence of dominant/persistent noise sources remains a possible origin of highly asymmetric correlation peaks [*Stehly et al.*, 2006; *Yang and Ritzwoller*, 2008]. In other words, careful surveys of dominant and/or persistent noise sources may be necessary prior to tomographic imaging.

[4] So far, asymmetric noise correlation functions at microseismic frequencies (5–20 s) have been attributed to ground motion caused by ocean swells and coastal impact [*Longuet-Higgins*, 1950; *Gutenberg*, 1951]. These modest (in comparison with earthquakes >Mw 5) but persistent sources sometimes exhibit strong directivity and seasonal variations [e.g., *Schulte-Pelkum et al.*, 2004; *Shapiro et al.*, 2005; *Sabra et al.*, 2005a; *Gu et al.*, 2007; *Yang and Ritzwoller*, 2008]. A prime example is the coast of California, where strong current from the Pacific Ocean and a dense seismic network nearby combined to produce some of the best-seen, asymmetric noise cross-correlations to date [e.g., *Sabra et al.*, 2005b; *Gerstoft and Tanimoto*, 2007]. The effects of noise sources may potentially reach great distances as, for instance, the Gulf of Guinea and North Fiji Basin have been recently cited as potential global seismic noise sources [*Shapiro et al.*, 2006].

[5] With few exceptions [e.g., *Shapiro et al.*, 2006; *Stehly et al.*, 2006; *Yang and Ritzwoller*, 2008], there is generally a greater emphasis on characterizing the observed noise records and less on source modeling. Data characterization is fairly reliable for regions with relatively simple coastal geometries, for example, the coast of California where strong noise sources are expected to arrive from westerly directions. In comparison, mapping dominant noise sources in regions as complex as southern Italy requires more than a solid understanding of data alone; carefully designed numerical experiments and improved knowledge of the source distribution/effects in the study region may be necessary. This study is motivated by an initial analysis of seismic array data [*Gu et al.*, 2007, hereinafter referred to as Gu07] that reported robust noise sources near southern Italy using stacked correlation functions (Figure 1). Our main objective in this study is to combine improved data processing techniques with forward modeling of asymmetric noise sources to validate the proposed sources in this region. Our results lend further support for Gu07 and highlight the effectiveness of migration and forward modeling techniques in the analysis of seismic noise. For completeness we provide the details of the processing methodologies below despite a slight overlap with that former study.

2. Data and Method

[6] The main data set consists of broadband vertical-component seismic records from the Calabrian-Apennine-Tyrrhenian/Subduction-Collision-Accretion Network (CAT/SCAN) deployment for the months of August through September of 2004. We clip continuous displacement seismograms into hour-long segments and remove time windows containing known M > 5 earthquakes. We use one-bit normalized traces [*Bensen et al.*, 2007], in contrast with the original data (see Gu07), to minimize the potential influence of small-magnitude regional earthquakes. We then cross-correlate the hour-long bit streams for each station pair and stack the results to increase the signal-to-noise ratio (SNR). Since the cross-correlation stacking approach provides n^2 combinations, where n is the number of stations used (in our case n = 36), we obtain a total of 1296 cross-correlation functions for further source analysis.

[7] The optimal frequency range for our study is determined by a frequency-amplitude analysis. Cross-correlation stacks filtered using corner frequencies of 0.06–0.1 Hz, a frequency range containing possible signals from ocean-seafloor interactions [*Longuet-Higgins*, 1950], provides the most robust noise signals. Weaker signals are observed for the frequency band (0.03–0.06 Hz), and a high-frequency range containing "secondary" microseisms (0.1–0.3 Hz [*Longuet-Higgins*, 1950]) returns incoherent stacking results. Hence, the remainder of this analysis will concentrate on

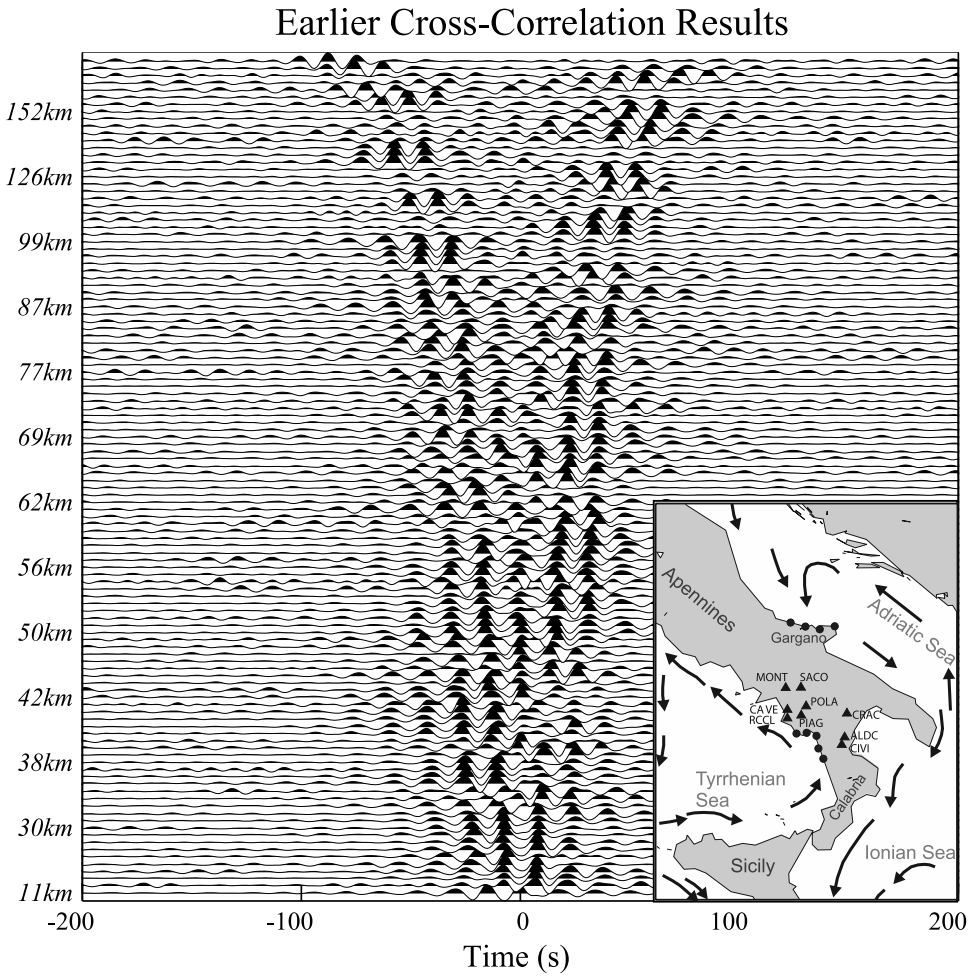

Figure 1. Cross-correlation stacks, arranged according to increasing station separation distances, of all station pairs from the CAT/SCAN deployment that satisfy SNR > 10. The map inset shows the general ocean current flow patterns during the study period and the inferred noise source locations by *Gu et al.* [2007].

"primary" microseismic frequencies where noise can be readily assessed and modeled.

[8] A number of different methods have been used previously in locating dominant noise sources. Examples include grid search misfit [*Shapiro et al.*, 2006] and mean stacked amplitude [*Rhie and Romanowicz*, 2006] algorithms and back projection [*Stehly et al.*, 2006; *Yang and Ritzwoller*, 2008]. We introduce a migration approach based on the equation below:

$$A(v,x,y) = \frac{1}{M*N}\sum_{j}^{M}\sum_{i}^{N} S\left(\frac{d_i(x,y) - d_j(x,y)}{v}\right) \quad (1)$$

where M and N are the number of stations (M is equal to 1 if the migration is performed on a single station), S is the Hilbert transform of the cross-correlation between stations i and j, and d represents the distance between the hypothetical source (with latitude x and longitude y) and station locations. The source-station distance is divided by v, the best fit regional velocity, to produce the predicted arrival time of the potential source. Figure 2 demonstrates the migration algorithm using two hypothetical source locations and a migration velocity of 3 km/s. Constructive interference due to the superior alignment of correlation peaks produces a higher migration amplitude at source location 1 than at source location 2.

[9] Our migration approach is a full-waveform method most similar to the mean stacked amplitude grid search algorithm of *Rhie and Romanowicz* [2006]. The main difference is in the applications: we apply the migration method to cross-correlation functions between stations, whereas the earlier study focused on the original displacement/velocity seismograms from individual stations. Our method does not require travel time picks for misfit calcu-

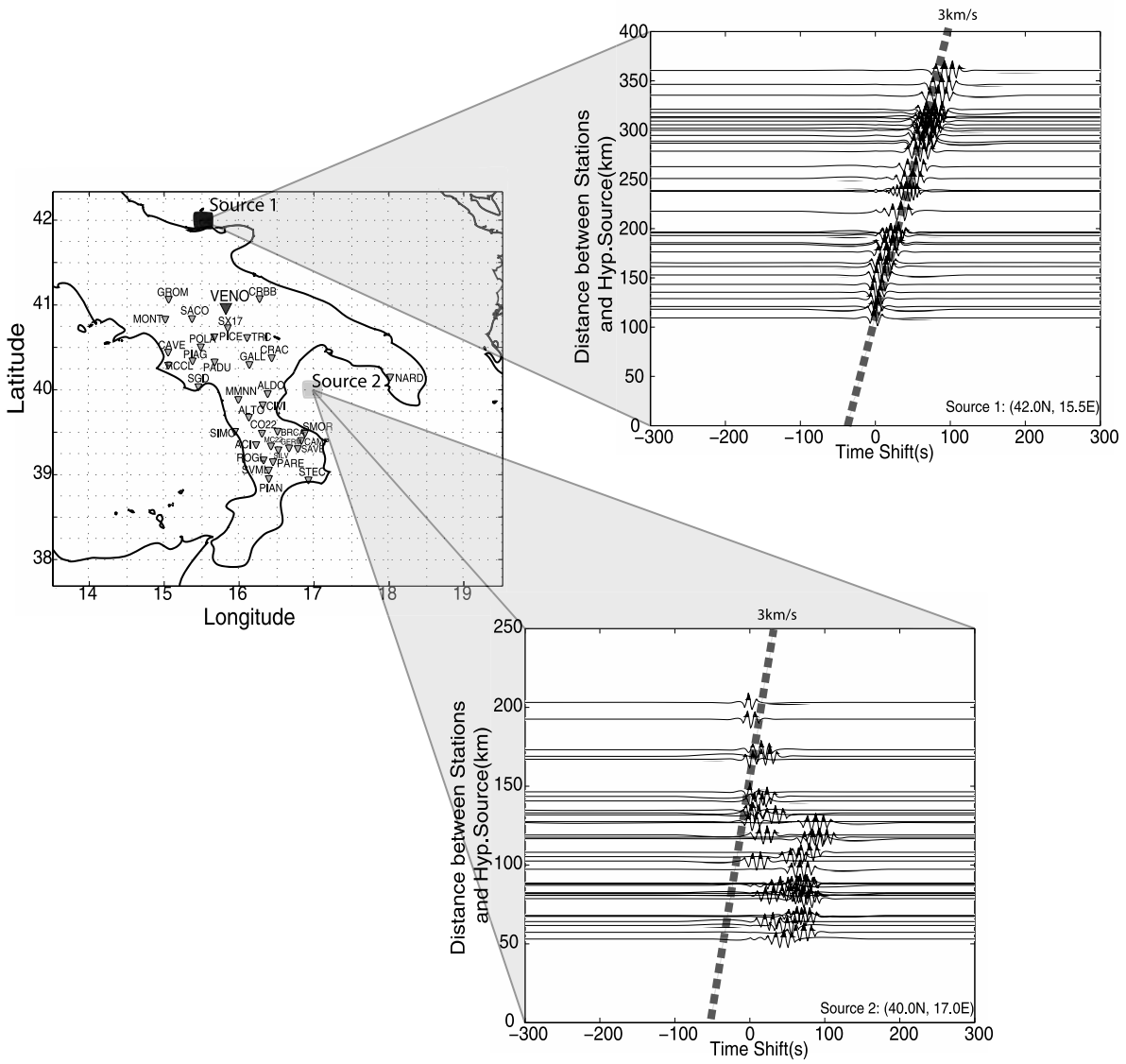

Figure 2. A demonstration of the source migration process using synthetic correlation functions. The original seismograms are computed by assuming a "true" source at (42°N, 15.5°E) and an average migration velocity of 3.0 km/s. The map on the left-hand side shows the stations used in this study. The correlation stacks with station VENO are used to compute migration amplitudes at two locations. For a possible source located near the true source (e.g., Source 1), the theoretical arrival times of Rayleigh waves accurately capture the moveout of correlation peaks and constructive interference leads to high migration amplitude (dark colors on the map). In contrast, a hypothetical source location away from the true source (e.g., Source 2) causes mismatches in arrival times (or correlation peak locations) and a low migration amplitude.

lation, a key difference with the grid search misfit algorithm of *Shapiro et al.* [2006].

[10] We account for the dependence of equation (1) on the input velocity model v by migrating the cross-correlation functions over a wide range of possible velocities (1.5–4 km/s). For each candidate velocity, the migration amplitude A (see equation (1)) of the entire study area (in our case, containing 250 × 250 possible source locations) is computed using all 36 cross-correlations with a common station. We then sum the resulting migration maps of A for all 36 stations (one map per station) and define the absolute maximum value of the summation as the Cumulative Migration Amplitude (CMA). A single value of CMA is obtained for each trial velocity v, and the velocity that produces the largest CMA is selected as the optimal regional velocity.

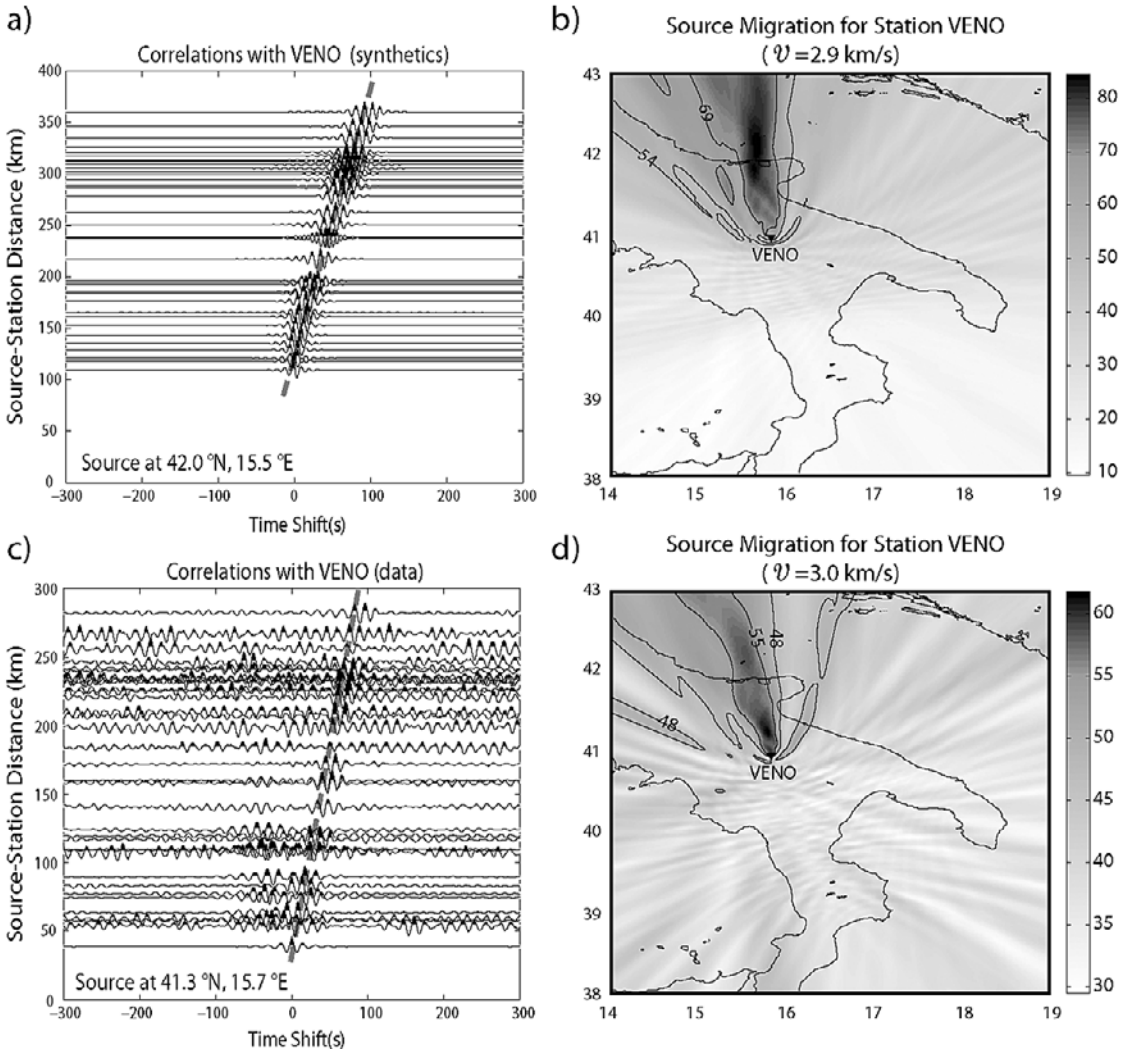

Figure 3. (a) Synthetic cross-correlations with station VENO, positioned according to their distances from the assumed (''true'') source location of (42°N, 15.5°E). The displacement synthetic seismograms are computed based on (1) an explosive source and (2) a migration velocity of 2.9 km/s. (b) Migration amplitude for the entire study region using the synthetic correlations. The hypothetical source location is correctly recovered by the global maxima of migration amplitudes (see dark-colored cells). The amplitude scale range is the percentage of maximal migration amplitude. (c) The observed cross-correlation stacks for station VENO, arranged by distance from the optimal source migration location. (d) The optimal source location based on correlations with station VENO. The experimentally determined migration velocity (see main text) is 3.0 km/s.

[11] To validate the migration results we conduct a qualitative comparison of noise cross-correlations with those reconstructed based on a series of source geometries/mechanisms. For simplicity, the surface waves produced by each potential point source are approximated by a Ricker wavelet with a center frequency of 0.08 Hz (12.5 s) and zero phase [e.g., *Campillo and Paul*, 2003]. The travel times of these wavelets are computed based on the average migration velocity for the entire study region. We also incorporate the effect of geometrical spreading and the final synthetic waveform at each station location is constructed by summing the wavefield of all presumed sources.

3. Result

3.1. Source Migration

[12] To test the stability of our migration algorithm, we compute synthetic seismograms [*Kennett*, 1975; *Kind*, 1976] for all stations, assuming the one-dimensional (1-D) regional velocity model of A. Ökeler et al. (Seismic structure of the southern

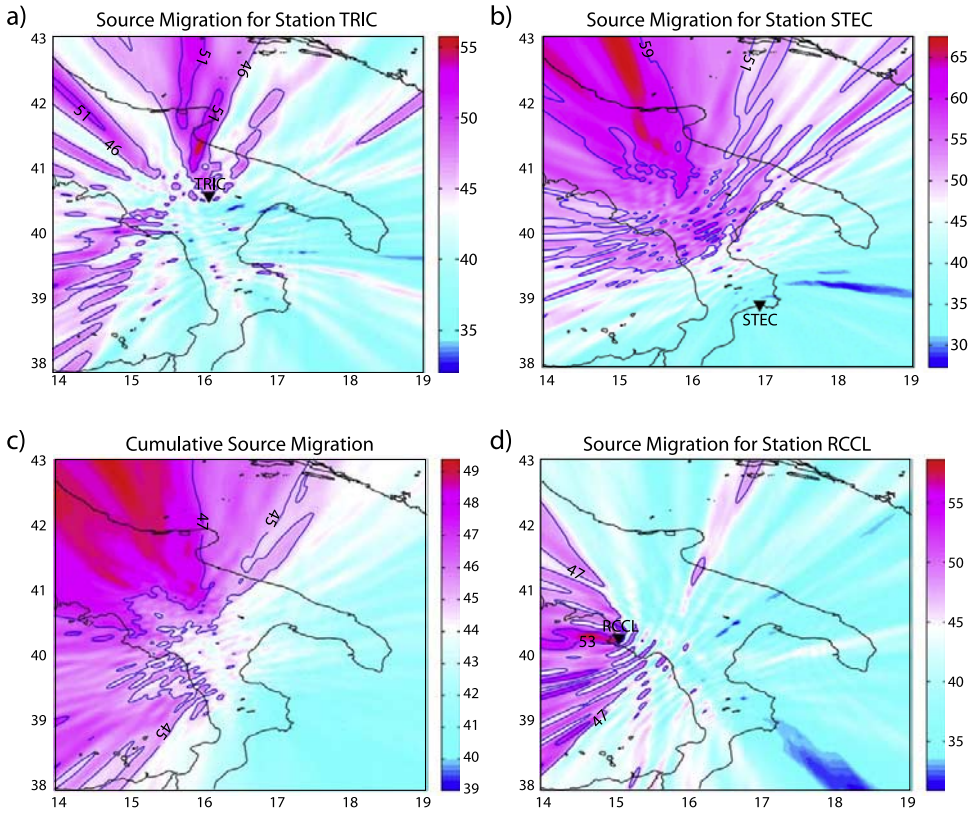

Figure 4. Sample source migration results based on correlations with the anchor stations (a) TRIC and (b) STEC. Both maps show maximum migration amplitudes north of the station array. (c) Cumulative source migration results from all stations. The optimal source location can be inferred from the high amplitude region northwest of the station array. (d) Migration map based on RCCL, a typical coastal station near the Tyrrhenian Sea. The location of maximum amplitude indicates a secondary source may be present along the Tyrrhenian Sea coast. Color scales are the same as Figures 3b and 3c.

Apennines, manuscript in preparation, 2009) and a hypothetical explosive source at (42°N, 15.5°E). These seismograms are filtered to the same frequency range as the observed noise records, and the resulting cross-correlations are migrated over a grid of potential source locations bounded by (38°N, 14°E) and (43°N, 19°E) and spaced by 0.02°. Figure 3a shows the synthetic cross-correlations for station VENO, arranged by distance from the presumed source location. The asymmetric moveout is similar to that shown by Gu07, despite a significantly smaller number of stations used in that earlier study. The migrated source location according to the strongest migration amplitude falls within ~0.2° of the latitude and longitude of the expected source (Figure 3b). The considerable scatter from the recovered source location along the north-south direction (pointing away from the station array) underscores the diminished sensitivity of cross-correlations to incoming waves from further distances along similar azimuths. Some of the differences between the original and recovered source locations may have resulted from the use of a homogeneous starting model for the migration procedure.

[13] The migration velocity of 3.0 km/s produces the highest CMA for the CAT/SCAN data set. This value is consistent with reported shallow crustal velocities of the southern Apennines in both earthquake-based (2.8–3.0 km/s (Ökeler et al., manuscript in preparation, 2009)) and noise-based (2.5–3.1 km/s [*Yang et al.*, 2007]) studies. The noise correlation stacks, which are aligned according to the station distance from the optimal migrated source location (Figures 3c and 3d), show asymmetric Rayleigh wave arrivals with a constant group velocity similar to that of the theoretical calculations (see Figure 3a). Despite slight ambiguities along the north-south orientation (see Figure 3d), the migrated sources consistently reside north of the CAT/SCAN stations for migration velocities between 2.0 km/s and 3.5 km/s.

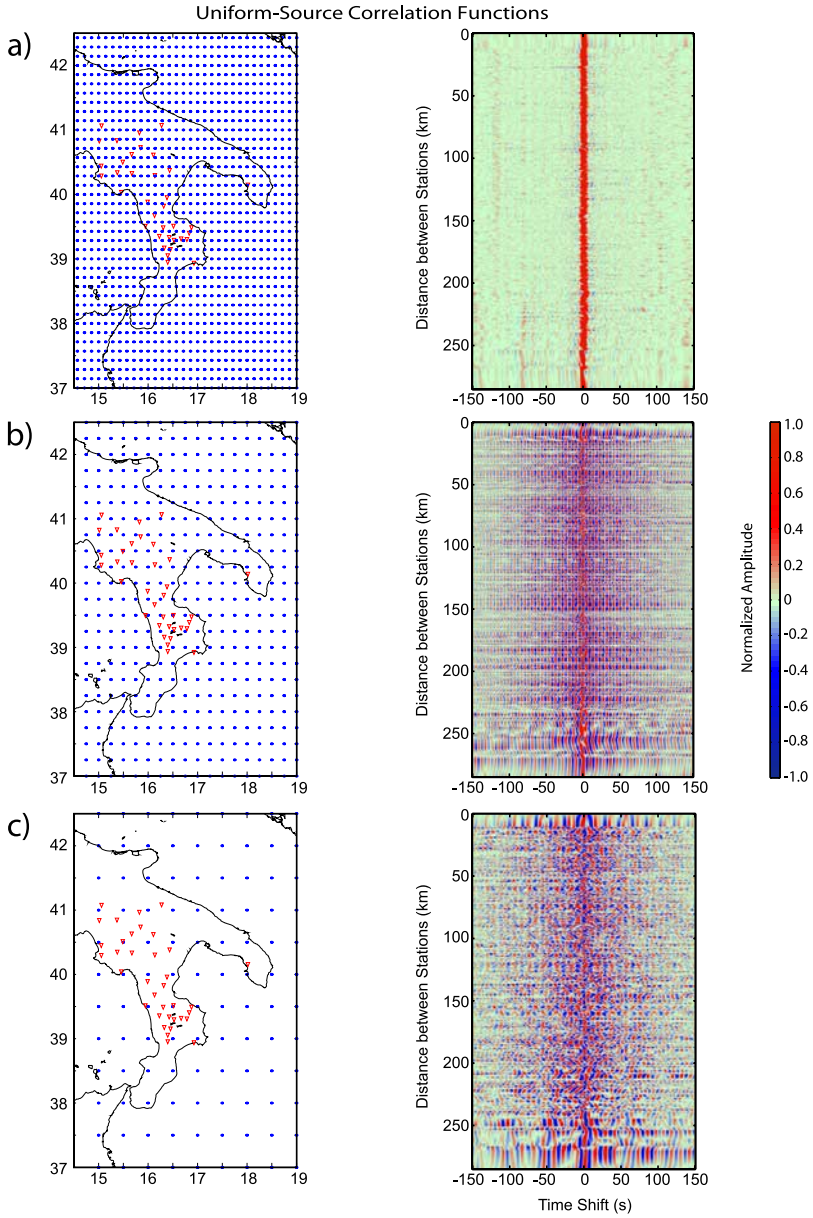

Figure 5. (right) Theoretical cross-correlation functions resulting from (left) simultaneously initiating sources for (a) 1600, (b) 400, and (c) 100 uniformly distributed sources. The source and station locations are represented by asterisks and triangles, respectively. Note: not all sources are within the displayed region.

[14] Migration results based on correlations with a common station (from here on, anchor station) (Figure 4) show nonuniform, dominant source orientations from the north/northwest and west/southwest of the CAT/SCAN array. Stations TRIC and STEC (Figures 4a and 4b) typify stations away from the Tyrrhenian coast that exhibit strong migration amplitudes in the north and northwest of the array. The inferred peak locations vary spatially depending on the anchor station during the migration process, though most appear to reside along the coastal regions of the Adriatic Sea at latitudes above 41°N. To a certain extent the output migration patterns are affected by the choice of anchor stations. For a set of fixed sources, the different responses of two anchor stations to each source is controlled by the source strength, station-source distances, path velocities, attenuation and other potential factors. Hence different anchor stations (e.g., TRIC and STEC) can have distinct source locations (see Figure 4). The size of the "cone-like" migration pattern around the maximum

reflects the uncertainty of the source locating process. For instance, the source position is better resolved by station TRIC than by station STEC, primarily due to a shorter distance from the former station to the source. The CMA from all stations (Figure 4c), defined as the average migration amplitude of 36 migration maps (one for each anchor station) at the same geographical location, presents the most convincing evidence for a non-uniform noise source. The global maximum roughly coincides with the Gargano promontory and the high amplitude zone extends laterally along the coastlines of northern Adriatic Sea. The orientation of this noise source is consistent with earlier results obtained by Gu07.

[15] A minor noise source is also present on the migration images of individual stations or groups of stations. For example, the migration stacks based on anchor station RCCL (Figure 4d) contains several local minima along the coastlines of the eastern Tyrrhenian Sea. These characteristics are typical of the source migration stacks from stations close to the Tyrrhenian coast (e.g., CAVE, SGIO, and SIMO), which may be caused by a secondary source first documented in the time-distance analysis of a northeast-southwest station transect (Gu07; see Figure 1 inset). The migration approach above provides first-order data constraints on two possible noise source locations. The section below verifies these sources through forward modeling of possible source distributions and geometries.

3.2. Forward Modeling of Noise Sources

[16] Four distinct types of source geometries and distributions are examined based on simulations of potential sources in and around southern Italy. The objective is to reproduce the environment under which asymmetric noise correlation peaks (see Figure 1) are generated. The first two types, randomly distributed and uniformly gridded sources are designed to mimic diffuse wavefields, or ambient noise, in the study region. The remaining two types, semicircular source distributions (case 3) and point sources (case 4), target the local geography of southern Italy and the two proposed source locations based on the migration analysis. All sources are assumed to initiate simultaneously, a condition that is somewhat subjective, but necessary without detailed information on the nature of the noise sources. Furthermore, the order of correlation between any given station pair is determined alphabetically based on the station name, and redundancies due to station order reversal in the pairing process are removed.

[17] Figure 5 shows three different grids of uniformly spaced sources and their resulting cross correlations, ordered according to the distance between each station pair. The underlying hypothesis is that properly chosen noise distribution should produce correlation stacks similar to the observations presented in Figure 1, albeit at a linear distance scale. However, the main characteristics of simulated and observed correlations differ substantially. In particular, theoretical correlations based on a uniform source distribution fail to produce meaningful moveout curves apart from a modest correlation peak at zero time lag. The strength of the zero lag correlation peak appears to depend on the density of the sources, as increase grid spacing tends to focus the cross-correlation amplitudes toward zero lag time.

[18] We observe a similar outcome to that of the uniform source patterns from random source distributions. In this case, we use a random generator to place sources near the Italian Peninsula (Figure 6) and the cross-correlation functions consistently show little, if any, coherent signals away from zero lag time. In fact, as suggested by Figures 5a and 6a, results from the random source distribution becomes nearly equivalent to those of evenly spaced sources when the number of sources increases. Neither type of source geometries adequately explains the apparent moveout of correlation peaks shown by Figure 1.

[19] The two remaining cases customize source geometries by incorporating known information on the geographical setting of the study region. For instance, it is natural to examine source geometries that capture the elongated shapes of the peninsula and station formation. The result of a circular source distribution around the peninsula (Figure 7a) shows visible improvement over uniform and random distributions. The correlation peaks no longer center on zero lag time for distances >75 km. However, the amplitude and arrival times of the correlation peaks remain problematic: for instance, the apparent velocity of the correlation peaks of 5 km/s is ~2 km/s faster than the reported average crustal velocity of the region [*Yang et al.*, 2007]. These discrepancies persist after we densify the source array or alter the size/shape of the circular geometry.

[20] Sources along the irregular coastlines (Figure 7b) or near the center of the circle/station array (Figure 7c) produce correlation patterns that are

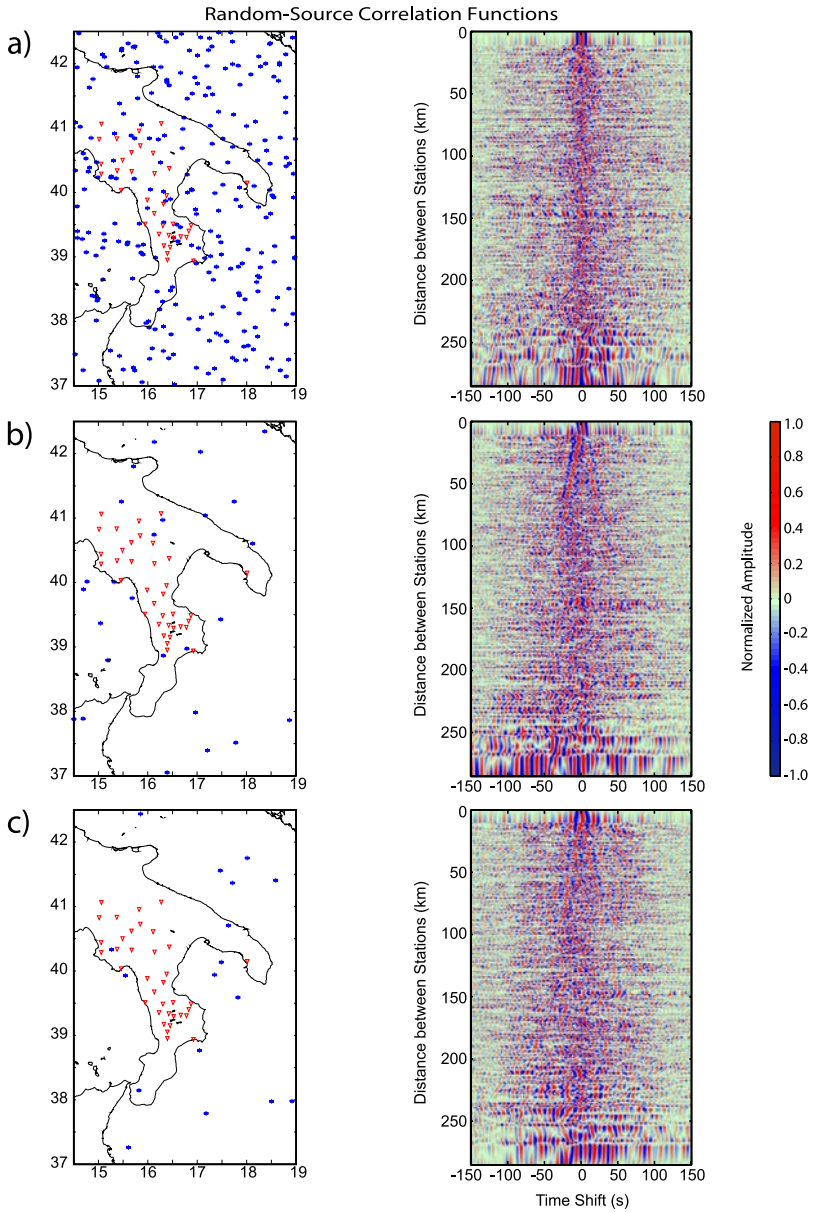

Figure 6. (right) Theoretical cross-correlations for (left) (a) 1000, (b) 100, and (c) 50 randomly distributed sources. The plot conventions are the same as Figure 5.

no closer to the "ground truth" (see Figure 1) than the geometries examined earlier. There is certain similarity, despite obvious differences in SNR, between the outputs of these two source scenarios (see Figures 7b and 7c). For instance, both correlation stacks contain weak but coherent signals for portions of the distance range. To a certain extent, a point source near the Gulf of Taranto (see Figure 7c) is close to an effective average of all sources along the complex coastlines (see Figure 7b).

[21] While a point source near the Gulf of Taranto fails to produce the correlations that match the observations, a point source (or a cluster of sources) north of the station array offers a viable solution to this problem (Figure 8). The outcome of a single explosive source near the Gargano promontory (Figure 8a) exhibits well-defined moveout curves. The apparent group speed of ~3.0 km/s is consistent with values obtained by migration (see section 3.1) and correlations (see Figure 1) of actual noise records. These correlation characteristics are preserved when additional sources are placed around Gargano (Figure 8b) and/or the eastern Tyrrhenian coast. The main difference in the outcomes of these source geometries (see Figures 8a–8c) is signal

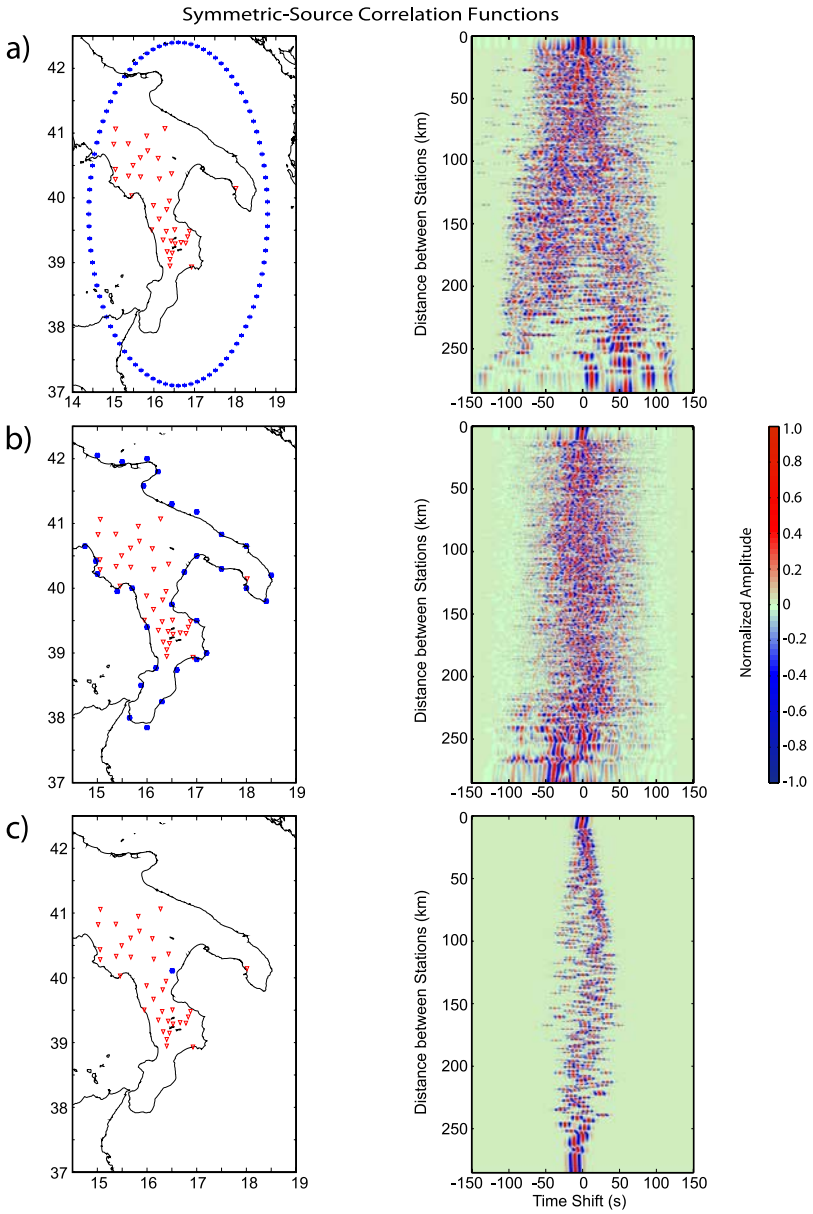

Figure 7. Similar to Figures 5 and 6, but for (a) semicircular and (b) coastal source distributions. The semicircular source distribution produces clear phase moveouts, but the inferred velocity is nearly twice as large as the observed. (c) Correlation stacks resulting from point source in the middle of the station array.

clarity: while multiple sources north of the station array tend to introduce unnecessary clutter in the correlation functions, the inclusion of a secondary source (Figure 8c) in the eastern Tyrrhenian Sea, assuming the same source strength, can introduce artifacts at distances <120 km and a shift of the correlation peaks toward zero lag time at long distances. Elimination of minor artifacts is possible for the latter two cases (see Figures 8b and 8c) via slight adjustments on the number of point sources, their locations, and source strengths. In other words, one or a combination of nonuniform source(s) properly positioned near the northern Adriatic and/or the Tyrrhenian coasts can sufficiently explain the dominant noise characteristics recorded by the CAT/SCAN station array.

3.3. Effect of Source Mechanism

[22] The noise source complexity involving ocean storms and infragravity waves have been well documented [*Schulte-Pelkum et al.*, 2004; *Rhie*

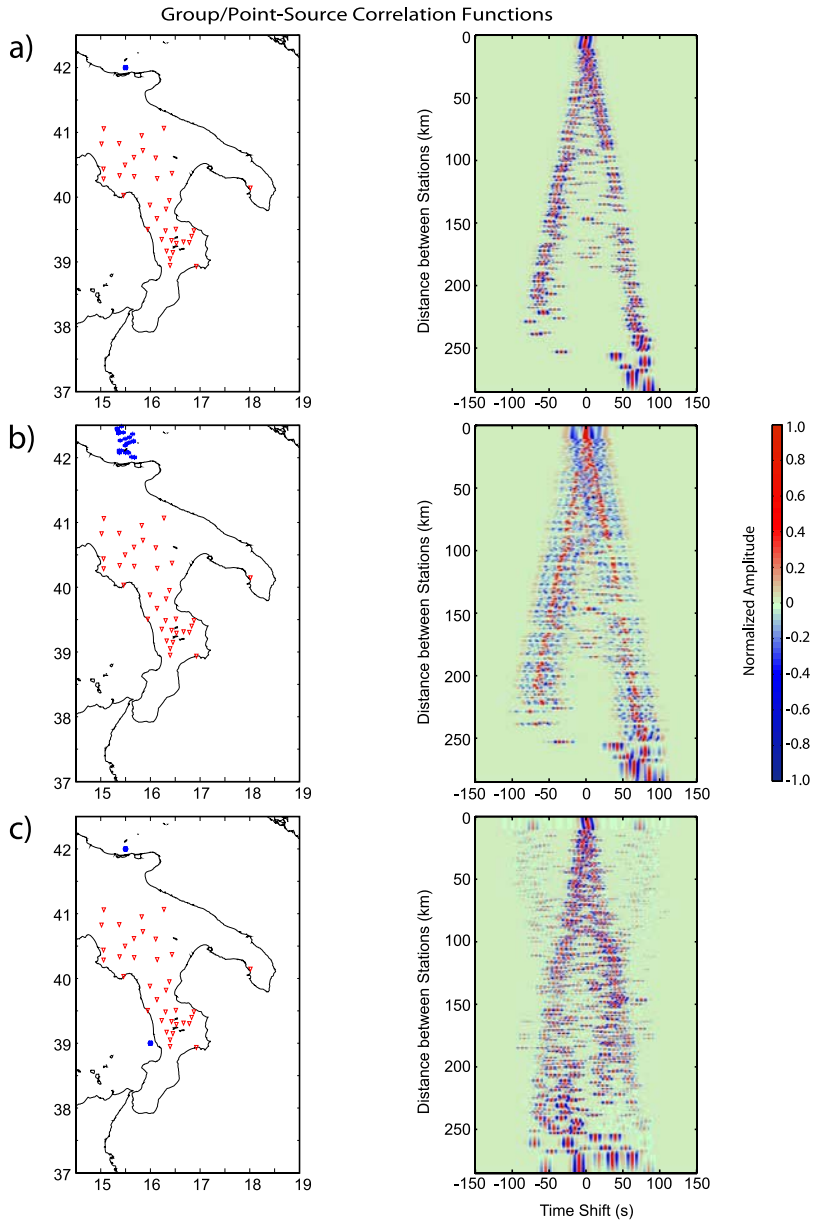

Figure 8. (a) Correlation functions resulting from a single source located off the Adriatic coast of southern Italy. (b) Similar to Figure 8a, but for multiple point sources (randomly distributed) that form a relative tight cluster in northern Adriatic Sea. (c) Results from two sources, one near the Gargano promontory and the other in the Tyrrhenian

and Romanowicz, 2006; *Gerstoft and Tanimoto*, 2007; *Webb*, 2007]. Without detailed knowledge of sources, our representation of atmosphere/ocean/seafloor coupling using an earthquake source mechanism is only a simplifying assumption. To test this assumption we compare the results of forward simulations by assuming various faulting geometries and mechanisms (Figure 9). Our experiments indicate that source mechanisms can occasionally cause significant Rayleigh wave amplitude and waveform complexities, as exemplified by the outcome of a 45° thrust mechanism (Figure 9c). That said, it is nearly impossible to differentiate a strike-slip (Figure 9b) from an explosive (Figure 3a) source mechanism based on the synthetic cross-correlations alone. The nonuniqueness is demonstrated further by a non-double-couple mechanism (Figure 9d) that is chosen to partially reflect the nonlinear nature of the source. The true source(s) likely depends on factors such as coastal

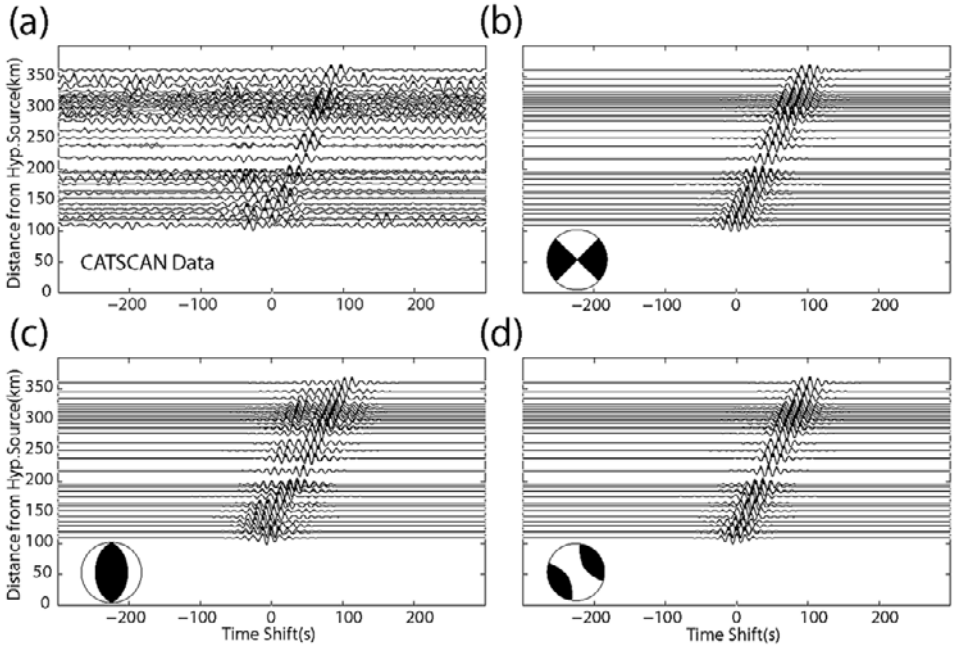

Figure 9. Effects of source mechanism on the cross-correlations based on anchor station VENO. (a) Correlation stacks based on two months of station records. Also shown are synthetic cross-correlations produced by (b) strike-slip, (c) thrust, and (d) non-double-couple source mechanisms. Synthetic cross-correlations are produced based on the 1-D regional velocity model of Ökeler et al. (manuscript in preparation, 2009).

geometry and bathymetry and may require a superposition of non-double-couple sources.

4. Discussion

[23] Effect of noise sources on the symmetry of correlation functions has been discussed in recent literatures through careful data processing [*Bensen et al.*, 2007] and source modeling [*Stehly et al.*, 2006; *Yang and Ritzwoller*, 2008] efforts. Under idealized source station geometry where dense and uniformly distributed (or, "ambient") noise sources are present, two symmetric correlation peaks relative to zero lag time are expected from forward waveform simulations [*Stehly et al.*, 2006]. A bias in source locations, on the other hand, can lead to an amplitude asymmetry in the causal and acausal halves of the resulting cross-correlations [*Stehly et al.*, 2006; *Yang and Ritzwoller*, 2008]. In reality, imperfections in noise source station geometry are the rule rather than the exception. Symmetry could be disrupted by small-magnitude earthquakes, by nonuniform global ocean distributions and their respective geometries and movements, as well as by complex atmosphere/ocean/seafloor coupling in the vicinity of the stations. Further complications have been documented, where both symmetric and asymmetric correlation peaks can result from nonuniform sources [*Yang and Ritzwoller*, 2008, Figures 13 and 14], depending on shape/orientation of the source and their relation to the station orientations. Our synthetic examples based on the available array geometry of CAT/SCAN stations (see Figures 5 and 6) demonstrate that correlation peaks with a positive, negative, and/or zero lag times could all result from relatively simple and uniform source distributions. Such complex behavior underscores the role of source balancing between one or several effective source(s) in noise correlation analysis.

[24] Our migration and forward waveform analyses consistently suggest effective noise sources from the north/northwest of the station array. The source orientation is well resolved based on the characteristics of the correlation peaks, but the existence of a distant "global" source [*Yang and Ritzwoller*, 2008] along the same orientation remains a possibility. The ambiguity of source location is further evidenced by a regional CAT/SCAN data migration (see section 2) over a global grid. The resulting CMA from all stations (Figure 10a) delineates spatially coherent maxima along a northwest trending, great circle path containing the station array. The migration amplitude reflects the probability of finding a persistent noise source at a given geographical location, a measure that predicates on the

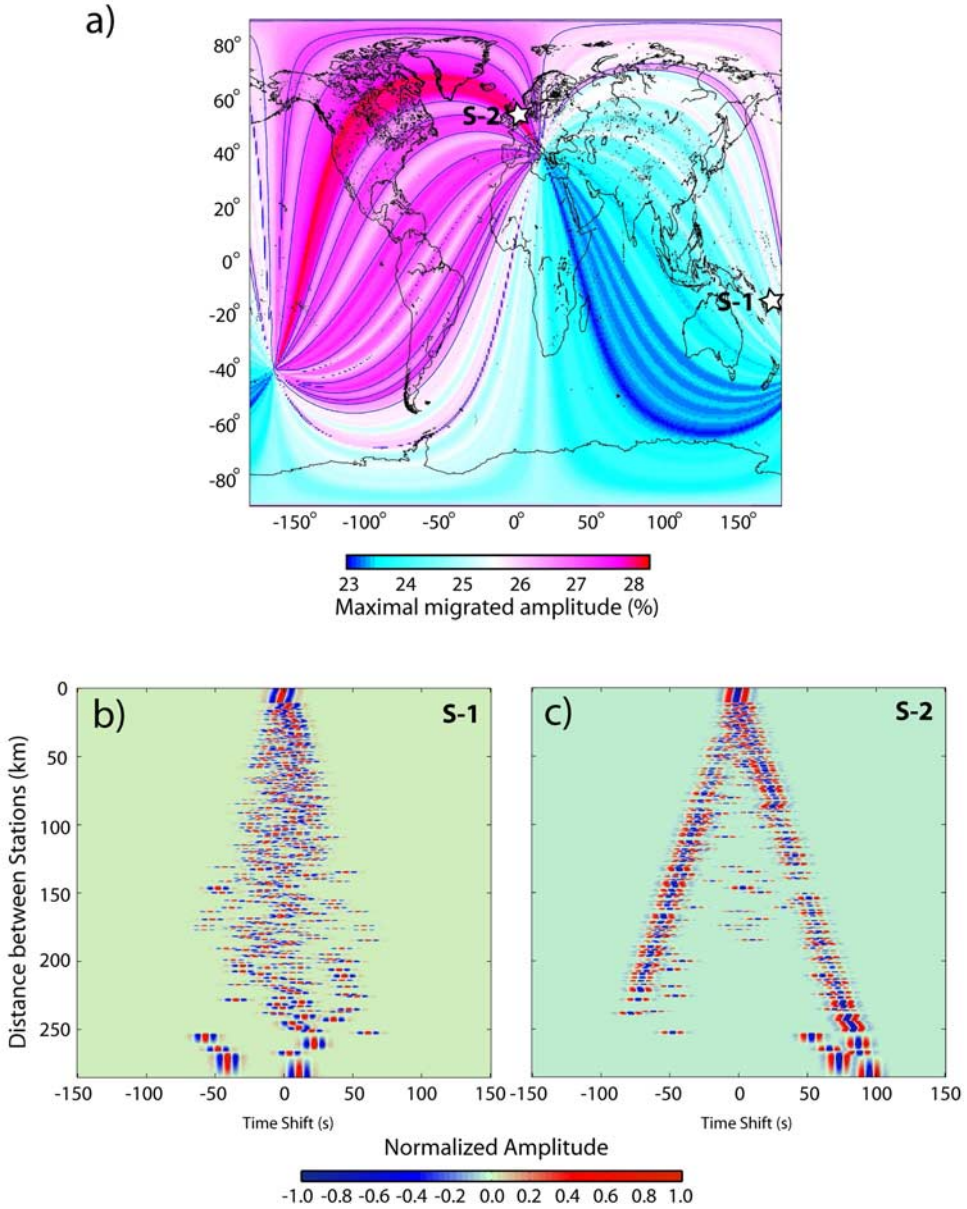

Figure 10. (a) Results from source migration for the entire globe using cross-correlations from August though September of 2004. The optimal noise sources, if global, reside in the Northern Hemisphere along a northwest-southeast great circle path across the station array (red colors). (b) Synthetic correlation functions computed based on a global noise source near Tonga island. (c) Synthetic correlation functions computed based on a global noise source near the Atlantic coast. Substantial differences in the clarity of the Rayleigh waves indicate that a potential source within the high-probability source path (see Figure 10a) is more difficult to differentiate from a regional noise source.

accuracy of distance-time description. For this reason noise sources away from the most probable great circle path should result in incoherent signals on the correlation stacks, a notion that is supported by the theoretical correlation functions associated with a hypothetical global noise source near Tonga (Figure 10b). For the same reason, the modest migration amplitudes in the southern hemisphere favors a regional/local source model, if one assumes that primary microsesimic noises predominantly originate from the southern hemisphere in summer months [*Yang and Ritzwoller*, 2008].

[25] The real challenge is to determine source location(s) within the high CMA band of a global migration map (see Figure 10a). Without detailed information on the strength of a noise source, the theoretical correlation peaks associated with a distant source (Figure 10c) can be nearly indistin-

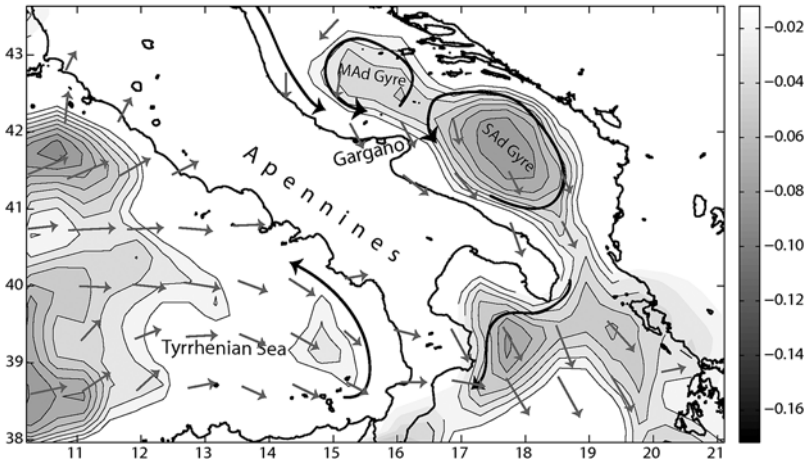

Figure 11. A map of southern Italy with typical ocean current flow patterns (dark arrows) and wind stress vectors (modified from *Zecchetto and De Biasio* [2007]). Contoured values represent the combined mean dynamic topography for the same region [*Rio et al.*, 2007] for the period of 1993–1999. Both studies show the long-term stability of the Mid-Adriatic (MAd), and South-Adriatic (SAd) gyres.

guishable from those of a nearby source (see Figures 8). Therefore, additional information on the strengths of the sources and the path attenuation structure would be necessary in assessing the precise location of source(s) along the northwest-southeast orientation. We conduct a synthetic migration analysis based on the PREM model [*Dziewonski and Anderson*, 1981], assuming a global source (see Figure 10a) and a secondary regional source near the Tyrrhenian source (see Figure 4d). In order to simultaneously recover the dominant northwest-southeast trending source orientation by inland stations (e.g., VENO, see Figures 3d) and a secondary source direction along the Tyrrhenian coast by coastal stations (e.g., RCCL, see Figure 4d), the energy of a presumed global source along the Atlantic coast must be 25–100 times larger than the local source due to surface wave attenuation. In comparison, the same data requirements can be easily met by a short-distance, regional source near the Gargano promontory. In other words, while we cannot rule out the effect of a global source, energy considerations and evidence from regional baroclinic estimates and dynamic topography models (see discussions below) make a regional source an appealing solution.

[26] The nature of coherent seismic noise is still debated, though the connection between detectable ground motion and ocean waves has been well documented for a wide range of frequencies. Earlier studies [*Longuet-Higgins*, 1950; *Gutenberg*, 1951] of background noise at microseismic frequencies attributed anomalous peak energies at 0.10–0.14 Hz to pressure variations caused by nonlinear interaction of ocean waves (primary) and coastal impact (secondary). The presence of coherent ambient noise was identified later through spectral analyses of normal modes [*Nawa et al.*, 1998; *Suda et al.*, 1998; *Tanimoto and Um*, 1999; *Ekström*, 2001], where dominant noise energies at ~0.004 Hz widely known as the Earth's hum were discovered. Noise peaks between these two frequency bands, for instance at ~26 s, also appear to be globally correlated with waves interacting with continental shelf [*Shapiro et al.*, 2006]. These frequency-dependent noise peaks could be caused by different mechanisms [*Webb*, 2007], though there is insinuating evidence that common near-coast excitation sources, most likely associated with atmosphere/ocean/seafloor coupling, could be responsible for noise correlation peaks at all frequencies [*Stehly et al.*, 2006; *Rhie and Romanowicz*, 2006; *Yang and Ritzwoller*, 2008].

[27] The migrated source location of persistent sources around southern Italy matches areas of strong local ocean currents impinging on coastal structures. Evidence of enhanced coastal interactions near the Gargano promontory was hypothesized by *Artegiani et al.* [1997] and supported by the reported baroclinic estimates of strong circulation velocities near the promontory as the greater gyre of the Adriatic deflects around the landmass. This finding is corroborated by drifter data [*Poulain*, 1999], from which surface motions of greater than 40 cm/s can be inferred in the vicinity of the Gargano promontory. Major reorganization of sediment pathways has also been documented in this

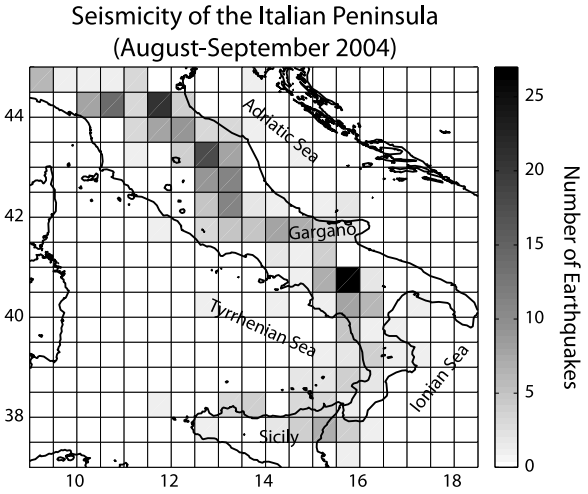

Figure 12. A map showing the frequency of earthquakes (M > 2) through the months of August and September of 2004. The region with the highest frequency of earthquakes (in the southern Apennines between 40.5° and 41°N and 15.5°–16°E) does not overlap with optimal source locations from migration analysis. The earthquake epicenters are taken from Italian Seismic Bulletin, Instituto Nazionale di Geofisica e Vulcanologia.

area in response to substantial sea level changes [*Steckler et al.*, 2007]. Figure 11 combines the reported flow directions [*Artegiani et al.*, 1997; *Poulain*, 1999] with a recent model of mean dynamic topography [*Rio et al.*, 2007] and mean wind stress vectors (modified from *Zecchetto and De Biasio* [2007]) in the Mediterranean Sea region (Figure 11). While the location(s) and mechanism(s) of coherent noise source(s) may not be unique, gravitational anomalies inferred from mean dynamic topography and substantial sea-wave activities near the Gargano promontory are certainly capable of generating detectable microseisms.

[28] Although one cannot rule out microearthquakes as possible noise sources beneath southern Italy, they are unlikely to be the dominant noise source in the vicinity of the Adriatic coast (the best source location) considering that during this time period, the majority of local seismicity occurs in the Apenninic mountain range (Figure 12). Further arguments can be made by the source migration result of VENO and RCCL (see Figures 3d and 4d, respectively), two nearby stations to the largest frequency of earthquakes for August–September 2004 that show a dominant source orientation away from the Apennines. We introduce an additional stability test of the migration imaging results using seven months (June through December, 2004) of vertical-component records at stations CRBB, GALL, GERM, and PADU (Figure 13); these are the only stations with uninterrupted recordings during this time range. The migrated source location (off the coasts of Adriatic Sea) is consistent with the earlier results shown by Figure 4c based on 2 months of data. In view of possible seasonal/monthly variations, the persistence of the main noise-correlation characteristics over time implies, at the shortest, an energetic noise source north of the station array during the summer of 2004.

5. Conclusions

[29] This study combines migration and forward source modeling techniques to validate the existence of persistent source location(s) in and around southern Italy. These techniques are commonly deployed in exploration seismology and earthquake-based analyses, but their applications in surveying noise sources have been relatively limited. The results of our study demonstrate that simple but effective noise source modeling is possible to verify the ''ambient source'' assumption prior to noise-based velocity analyses.

[30] Our experiments consistently suggest a dominant/persistent noise source near the Gargano promontory and a possible secondary source near the Tyrrhenian Sea coasts. Strong excitations in primary microseismic frequencies during the summer months of 2004 are likely responsible for coherent Rayleigh wave energies on the vertical-component records of broadband seismic stations

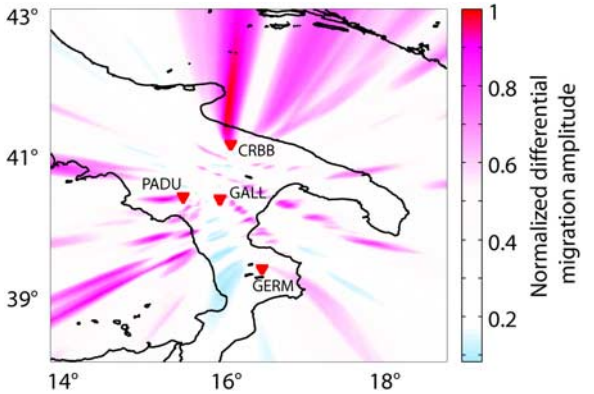

Figure 13. Source migration results for the months of June through December of 2004. The CMA are computed based on contributions from stations CRBB, GALL, GERM, and PADU. The optimal source location for the seven months of recordings (north of station CRBB and near the Gargano Promontory) is consistent with results shown by Figure 4.

in southern Italy. A point source or a cluster of point sources can adequately explain the coherent noise signals, while inconsistencies in correlation amplitudes and moveouts argue against a uniform or random distribution of point sources. The nature of the proposed noise sources is still uncertain, but buoy records, baroclinic estimates, and dynamic topography models provide extensive evidence that link these sources to ocean storms and heightened wave interactions off the Adriatic coasts of the Italian Peninsula. Future work will be needed to accurately determine the precise mechanisms by which the coherent noise sources are generated in southern Italy.

Acknowledgments

[31] We wish to thank the CAT/SCAN team for the acquisition of the data set for our analysis and IRIS DMS for the data archival and dissemination. We acknowledge the help of the institutions of NOAA, NASA, and Mercator Operational Oceanography for information and data on dynamic ocean topography. This research is funded by from National Science and Engineering Council (NSERC), Alberta Ingenuity, Canadian Foundation for Innovation (CFI), and the Roy Dean Hibb's Memorial Scholarship.

References

Artegiani, A., D. Bregant, E. Paschini, N. Pinardi, F. Raicich, and A. Russo (1997), The Adriatic Sea general circulation. Part II: Baroclinic circulation structure, *J. Phys. Oceanogr.*, *27*(8), 1515–1532, doi:10.1175/1520-0485(1997)027<1515:TASGCP>2.0.CO;2.

Bensen, G. D., M. H. Ritzwoller, M. P. Barmin, A. L. Levshin, F. Lin, M. P. Moschetti, N. M. Shapiro, and Y. Yang (2007), Processing seismic ambient noise data to obtain reliable broad-band surface wave dispersion measurements, *Geophys. J. Int.*, *169*(3), 1239–1260, doi:10.1111/j.1365-246X.2007.03374.x.

Campillo, M., and A. Paul (2003), Long-range correlations in the diffuse seismic coda, *Science*, *299*(5606), 547–549, doi:10.1126/science.1078551.

Cho, K. H., R. B. Herrmann, C. J. Ammon, and K. Lee (2007), Imaging the upper crust of the Korean Peninsula by surfacewave tomography, *Bull. Seismol. Soc. Am.*, *97*(1B), 198–207, doi:10.1785/0120060096.

Claerbout, J. (1968), Synthesis of a layered medium from its acoustic transmission response, *Geophysics*, *33*(2), 264–269, doi:10.1190/1.1439927.

Dziewonski, A. M., and D. L. Anderson (1981), Preliminary reference Earth model, *Phys. Earth Planet. Inter.*, *25*(4), 297–356.

Ekström, G. (2001), Time domain analysis of the Earths background seismic radiation, *J. Geophys. Res.*, *106*, 26,483–26,494, doi:10.1029/2000JB000086.

Gerstoft, P., and T. Tanimoto (2007), A year of microseisms in southern California, *Geophys. Res. Lett.*, *34*, L20304, doi:10.1029/2007GL031091.

Gu, Y. J., C. Dublanko, A. Lerner-Lam, K. Brzak, and M. Steckler (2007), Probing the sources of ambient seismic noise near the coasts of southern Italy, *Geophys. Res. Lett.*, *34*, L22315, doi:10.1029/2007GL031967.

Gudmundsson, O., A. Khan, and P. Voss (2007), Rayleigh-wave group velocity of the Icelandic crust from correlation of ambient seismic noise, *Geophys. Res. Lett.*, *34*, L14314, doi:10.1029/2007GL030215.

Gutenberg, G. (1951), Observation and theory of microseisms, in *Compendium of Meteorology*, edited by T. F. Malone, pp. 1303–1311, Am. Meteorol. Soc., Boston, Mass.

Kennett, B. L. N. (1975), The effect of attenuation on seismograms, *Bull. Seismol. Soc. Am.*, *65*, 1643–1651.

Kind, R. (1976), Computation of reflection coefficients for layered media, *J. Geophys.*, *42*, 191–200.

Kunetz, G., and I. d'Erceville (1962), Sur certaines proprieties d'une onde acoustique plane de compression dans un milieu stratifie, *Ann. Geophys.*, *18*, 351–359.

Lin, F. C., M. H. Ritzwoller, J. Townend, S. Bannister, and M. K. Savage (2007), Ambient noise Rayleigh wave tomography of New Zealand, *Geophys. J. Int.*, *170*, 649–666, doi:10.1111/j.1365-246X.2007.03414.x.

Lin, F. C., M. P. Moschetti, and M. H. Ritzwoller (2008), Surface wave tomography of the western United States from ambient seismic noise: Rayleigh and Love wave phase velocity maps, *Geophys. J. Int.*, *173*, 281–298, doi:10.1111/j.1365-246X.2008.03720.x.

Lobkis, O., and R. Weaver (2001), On the emergence of the Greens function in the correlations of a diffuse field, *J. Acoust. Soc. Am.*, *110*(6), 3011–3017, doi:10.1121/1.1417528.

Longuet-Higgins, M. S. (1950), A theory on the origin of microseisms, *Philos. Trans. R. Soc. London, Ser. A*, *243*(857), 1–35, doi:10.1098/rsta.1950.0012.

Moschetti, M. P., M. H. Ritzwoller, and N. M. Shapiro (2007), Surface wave tomography of the western United States from ambient seismic noise: Rayleigh wave group velocity maps, *Geochem. Geophys. Geosyst.*, *8*, Q08010, doi:10.1029/2007GC001655.

Nawa, K., N. Suda, Y. Fukao, T. Sato, Y. Aoyama, and K. Shibuya (1998), Incessant excitation of the Earths free oscillations, *Earth Planets Space*, *50*(1), 3–8.

Poulain, P. M. (1999), Drifter observations of surface circulation in the Adriatic Sea between December 1994 and March 1996, *J. Mar. Syst.*, *20*, 231–253, doi:10.1016/S0924-7963(98)00084-0.

Rhie, J., and B. Romanowicz (2006), A study of the relation between ocean storms and the Earths hum, *Geochem. Geophys. Geosyst.*, *7*, Q10004, doi:10.1029/2006GC001274.

Rickett, J., and J. Claerbout (1999), Acoustic daylight imaging via spectral factorization: Helioseismology and reservoir monitoring, *Lead. Edge*, *18*, 957–960, doi:10.1190/1.1438420.

Rio, M.-H., P.-M. Poulain, A. Pascual, E. Mauri, G. Larnicol, and R. Santoleri (2007), A mean dynamic topography of the Mediterranean Sea computed from altimetric data, in-situ measurements and a general circulation model, *J. Mar. Syst.*, *65*, 484–508, doi:10.1016/j.jmarsys.2005.02.006.

Roux, P., K. G. Sabra, P. Gerstoft, W. A. Kuperman, and M. C. Fehler (2005), P waves from cross-correlation of seismic noise, *Geophys. Res. Lett.*, *32*, L19303, doi:10.1029/2005GL023803.

Sabra, K. G., P. Gerstoft, P. Roux, and W. A. Kuperman (2005a), Extracting time-domain Greens function estimates from ambient seismic noise, *Geophys. Res. Lett.*, *32*, L03310, doi:10.1029/2004GL021862.

Sabra, K. G., P. Gerstoft, P. Roux, and W. A. Kuperman (2005b), Surface wave tomography from microseisms in

Southern California, *Geophys. Res. Lett.*, *32*, L14311, doi:10.1029/2005GL023155.

Schulte-Pelkum, V., P. S. Earle, and F. L. Vernon (2004), Strong directivity of ocean-generated seismic noise, *Geochem. Geophys. Geosyst.*, *5*, Q03004, doi:10.1029/2003GC000520.

Shapiro, N. M., M. Campillo, L. Stehly, and M. H. Ritzwoller (2005), High resolution surface wave tomography from ambient seismic noise, *Science*, *307*, 1615–1618, doi:10.1126/science.1108339.

Shapiro, N. M., M. H. Ritzwoller, and G. D. Bensen (2006), Source location of the 26 sec microseism from cross-correlations of ambient seismic noise, *Geophys. Res. Lett.*, *33*, L18310, doi:10.1029/2006GL027010.

Snieder, R. (2004), Extracting the Greens function from the correlation of coda waves: A derivation based on stationary phase, *Phys. Rev. E*, *69*(4), 046610, doi:10.1103/PhysRevE.69.046610.

Steckler, M. S., D. Ridente, and F. Trincardi (2007), Modeling of sequence geometry north of Gargano Peninsula by changing sediment pathways in the Adriatic Sea, *Cont. Shelf Res.*, *27*, 526–541, doi:10.1016/j.csr.2006.11.007.

Stehly, L., M. Campillo, and N. Shapiro (2006), A study of the seismic noise from its long-range correlation properties, *J. Geophys. Res.*, *111*, B10306, doi:10.1029/2005JB004237.

Suda, N., K. Nawa, and Y. Fukao (1998), Earths background free oscillations, *Science*, *279*(5359), 2089–2091, doi:10.1126/science.279.5359.2089.

Tanimoto, T., and J. Um (1999), Cause of continuous oscillations of the Earth, *J. Geophys. Res.*, *104*(B12), 28,723–28,740, doi:10.1029/1999JB900252.

Wapenaar, K., J. Thorbecke, and D. Draganov (2004), Relations between reflection and transmission responses of three-dimensional inhomogeneous media, *Geophys. J. Int.*, *156*, 179–194, doi:10.1111/j.1365-246X.2003.02152.x.

Webb, S. C. (2007), The Earths 'hum' is driven by ocean waves over the continental shelves, *Nature*, *445*, 754–756, doi:10.1038/nature05536.

Yang, Y., and M. Ritzwoller (2008), Characteristics of ambient seismic noise as a source for surface wave tomography, *Geochem. Geophys. Geosyst.*, *9*, Q02008, doi:10.1029/2007GC001814.

Yang, Y., M. H. Ritzwoller, A. L. Levshi, and N. M. Shapiro (2007), Ambient noise Rayleigh wave tomography across Europe, *Geophys. J. Int.*, *168*, 259–274, doi:10.1111/j.1365-246X.2006.03203.x.

Yao, H., R. D. van der Hilst, and M. V. De Hoop (2006), Surface-wave array tomography in SE Tibet from ambient seismic noise and two-station analysis: I—Phase velocity maps, *Geophys. J. Int.*, *166*, 732–744, doi:10.1111/j.1365-246X.2006.03028.x.

Zecchetto, S., and F. De Biasio (2007), Sea surface winds over the Mediterranean basin from satellite data (2000–04), meso- and local-scale features on annual and seasonal time scales, *J. Appl. Meteorol. Climatol.*, *46*, 814–827, doi:10.1175/JAM2498.1.